Facets of Uncertainty/STAHY 2013 | Kos Island, Greece, 17-19 October 2013 | Poster P-33

Simultaneous use of observations and deterministic model outputs to forecast persistent stochastic processes

H. Tyralis and D. Koutsoyiannis, Department of Water Resources and Environmental Engineering, National Technical University of Athens (itia.ntua.gr/1401)

1. Abstract

We combine a time series of a geophysical process with the output of a deterministic model, which simulates the aforementioned process in the past also providing future predictions. The purpose is to convert the single prediction of the deterministic model for the future evolution of the time series into a stochastic prediction. The time series is modelled by a stationary persistent normal stochastic process. The output of the deterministic model comprises of the simulation historical part of the process and its deterministic future prediction. The complexity of the deterministic model is assumed to be irrelevant to our framework. A multivariate stochastic process, whose first variable is the true (observable) process and the second variable is a process representing the deterministic model, is formed. The covariance matrix function is computed and the distribution of the unobserved part of the stochastic process is calculated conditional on the observations and the output of the deterministic model.

2. Definitions

We assume that $\{\underline{x}_{1t}\},\{\underline{x}_{2t}\}$, $t = 1, 2, \ldots$ are two Hurst-Kolmogorov stochastic processes (HKp) with means μ_1, μ_2, standard deviations σ_1, σ_2, autocovariance functions γ_{1k}, γ_{2k}, and autocorrelation functions (ACF) $\rho_{1k} := \gamma_{1k} / \sigma_1$, $\rho_{2k} := \gamma_{2k} / \sigma_2$, $(k = 0, \pm1, \pm2, \ldots)$.

Then the normal bivariate process $\{\underline{\boldsymbol{x}}_t = (\underline{x}_{1t},\underline{x}_{2t})\}$, $t = 1, 2, \ldots$ is a well-balanced HKp if (Amblard et al. 2012)

$$\gamma_{ij}(k) := \mathrm{Cov}[\underline{x}_{it}, \underline{x}_{j\,t+k}] = (1/2)\,\sigma_i\,\sigma_j\,\big(w_{ij}(k-1) - 2\,w_{ij}(k) + w_{ij}(k+1)\big) \text{ and } w_{ij}(k) := \rho_{i,j}\,|k|^{H_i+H_j},\ \rho_{i,i} = 1,\ \rho_{i,j} = \rho_{j,i} = \rho,\ (i,j) \in \{\{1,2\},\{1,2\}\} \tag{1}$$

under the restriction $\rho^2 \le \dfrac{\Gamma(2H_1+1)\,\Gamma(2H_2+1)\,\sin(\pi H_1)\,\sin(\pi H_2)}{\Gamma^2(H_1+H_2+1)\,\sin^2(\pi(H_1+H_2)/2)}$.

The problem of finding and assessing the maximum likelihood estimator for the parameters of the HKp was studied by Tyralis and Koutsoyiannis (2011). The solution of the same problem for the bivariate HKp is more complicated. We assume that there is a record of n observations $\boldsymbol{x}_{1\,1:n} := (x_{11} \ldots x_{1n})^{\mathrm{T}}$ and $\boldsymbol{x}_{2\,1:n} := (x_{21} \ldots x_{2n})^{\mathrm{T}}$. The parameters of the bivariate HKp are $\boldsymbol{\theta} = (\mu_1, \mu_2, \sigma_1, \sigma_2, H_1, H_2, \rho)$. We use the terminology of Wei (2006, p.382-427). Hence we have the mean vector $\mathrm{E}[\underline{\boldsymbol{x}}_t] = [\mu_1\ \mu_2]^{\mathrm{T}}$ and the lag-k covariance matrix function $\boldsymbol{\Gamma}(k)$:

$$\boldsymbol{\Gamma}(k) := \mathrm{Cov}[\underline{\boldsymbol{x}}_t, \underline{\boldsymbol{x}}_{t+k}] = \begin{bmatrix} \gamma_{11}(k) & \gamma_{21}(k) \\ \gamma_{21}(k) & \gamma_{22}(k) \end{bmatrix} \tag{2}$$

The covariance matrix of the multivariate normal variable $\underline{\boldsymbol{x}}_{1:n} := [\,\underline{\boldsymbol{x}}_1^{\mathrm{T}}\ \underline{\boldsymbol{x}}_2^{\mathrm{T}} \ldots \underline{\boldsymbol{x}}_n^{\mathrm{T}}\,]^{\mathrm{T}}$ is

$$\boldsymbol{\Gamma} = \begin{bmatrix} \boldsymbol{\Gamma}(0) & \boldsymbol{\Gamma}(1) & \ldots & \boldsymbol{\Gamma}(n-1) \\ \boldsymbol{\Gamma}(1) & \boldsymbol{\Gamma}(0) & \ldots & \boldsymbol{\Gamma}(n-2) \\ \ldots & \ldots & \ldots & \ldots \\ \boldsymbol{\Gamma}(n-1) & \boldsymbol{\Gamma}(n-2) & \ldots & \boldsymbol{\Gamma}(0) \end{bmatrix} \tag{3}$$

3. Maximum likelihood estimates

Rearranging the elements of $\underline{\boldsymbol{x}}_{1:n}$ we define the vector $\underline{\boldsymbol{w}}_{1:n} := [\underline{\boldsymbol{x}}_{1\,1:n}^{\mathrm{T}}\ \underline{\boldsymbol{x}}_{2\,1:n}^{\mathrm{T}}]^{\mathrm{T}}$ with covariance matrix

$$\boldsymbol{\Sigma} = \begin{bmatrix} \boldsymbol{\Sigma}_1 & \boldsymbol{\Sigma}_{12} \\ \boldsymbol{\Sigma}_{21} & \boldsymbol{\Sigma}_2 \end{bmatrix} \tag{4}$$

$$\boldsymbol{\Sigma}_1 := \sigma_1^2\,\boldsymbol{R}_1,\ [\boldsymbol{R}_1]_{(i,j)} = [\boldsymbol{R}_1]_{(j,i)} := \rho_{1(j-i)},\ \boldsymbol{\Sigma}_2 := \sigma_2^2\,\boldsymbol{R}_2,\ [\boldsymbol{R}_2]_{(i,j)} = [\boldsymbol{R}_2]_{(j,i)} := \rho_{2(j-i)},\ \boldsymbol{\Sigma}_{21} = \boldsymbol{\Sigma}_{12} := \rho_{12}\,\sigma_1\,\sigma_2\,\boldsymbol{R}_{21},\ [\boldsymbol{R}_{21}]_{(i,j)} = [\boldsymbol{R}_{21}]_{(j,i)} := \rho_{21}(j-i) \tag{5}$$

$$\rho_{21}(j-i) := \gamma_{21}(j-i) / (\rho\,\sigma_1\,\sigma_2) = (1/2)\,\big(\,|j-i-1|^{H_1+H_2} - 2\,|j-i\,|^{H_1+H_2} + |j-i+1|^{H_1+H_2}\,\big) \tag{6}$$

Now we define the vectors

$$\boldsymbol{e}_n = [\,1\ 1 \ldots 1\,]^{\mathrm{T}},\ \boldsymbol{\mu} = [\,\mu_1\boldsymbol{e}_n^{\mathrm{T}}\ \mu_2\boldsymbol{e}_n^{\mathrm{T}}\,]^{\mathrm{T}} \tag{7}$$

The probability distribution function of $\underline{\boldsymbol{w}}$ is

$$f(\underline{\boldsymbol{w}}_{1:n}) = (2\pi)^{-n}\,|\boldsymbol{\Sigma}|^{-1/2} \exp((\boldsymbol{w}_{1:n} - \boldsymbol{\mu})^{\mathrm{T}}\,\boldsymbol{\Sigma}^{-1}\,(\boldsymbol{w}_{1:n} - \boldsymbol{\mu})) \tag{8}$$

It is shown that

$$\hat{\sigma}_1 = ((a_1\,a_3^{1/2} - \rho\,a_2\,a_1^{1/2})/(\mathrm{n}\,a_3^{1/2}))^{1/2},\ \hat{\sigma}_2 = ((a_3\,a_1^{1/2} - \rho\,a_2\,a_3^{1/2})/(\mathrm{n}\,a_1^{1/2}))^{1/2} \tag{9}$$

where

$$a_1 := \boldsymbol{y}_{1\,1:n}^{\mathrm{T}}\,(\boldsymbol{R}_1 - \rho^2\,\boldsymbol{R}_{21}\,\boldsymbol{R}_2^{-1}\,\boldsymbol{R}_{21})^{-1}\,\boldsymbol{y}_{1\,1:n},\ a_2 := \boldsymbol{y}_{2\,1:n}^{\mathrm{T}}\,(\boldsymbol{R}_2 - \rho^2\,\boldsymbol{R}_{21}\,\boldsymbol{R}_1^{-1}\,\boldsymbol{R}_{21})]^{-1}\,\boldsymbol{R}_{21}\,\boldsymbol{R}_1^{-1}\,\boldsymbol{y}_{1\,1:n},\ a_3 := \boldsymbol{y}_{2\,1:n}^{\mathrm{T}}\,(\boldsymbol{R}_2 - \rho^2\,\boldsymbol{R}_{21}\,\boldsymbol{R}_1^{-1}\,\boldsymbol{R}_{21})^{-1}\,\boldsymbol{y}_{2\,1:n} \tag{10}$$

$$\boldsymbol{y}_{1\,1:n} = [\,\boldsymbol{x}_{1\,1:n}^{\mathrm{T}} - \mu_1\boldsymbol{e}_n^{\mathrm{T}}]^{\mathrm{T}},\ \boldsymbol{y}_{2\,1:n} = [\boldsymbol{x}_{2\,1:n}^{\mathrm{T}} - \mu_2\boldsymbol{e}_n^{\mathrm{T}}\,]^{\mathrm{T}} \tag{11}$$

Now substituting (9) in (8) and maximizing the three parameters log-likelihood we obtain $\hat{H}_1$, $\hat{H}_2$, $\hat{\rho}$. After substituting these values in (9) we obtain $\hat{\sigma}_1$ and $\hat{\sigma}_2$.

4. Posterior predictive distribution

We assume that $\boldsymbol{x}_{1\,1:(n+k)}$ is the output of the deterministic model and $\boldsymbol{x}_{2\,1:n}$ is the data observed. We wish to find the distribution of $\underline{\boldsymbol{x}}_{2\,(n+1):(n+m)}$ conditional on $\boldsymbol{x}_{1\,1:(n+m)}$ and $\boldsymbol{x}_{2\,1:n}$. Assuming that $\{\underline{\boldsymbol{x}}_t = (\underline{x}_{1t},\underline{x}_{2t})\}$, $t = 1, 2, \ldots$ is a bivariate HKp, the probability distribution of $\underline{\boldsymbol{w}}_{1:\,(n+m)}$ is given by (8). The $2(n+m)$-by-$2(n+m)$ covariance matrix of the process is given by (4) and is partitioned according to (12).

$$\boldsymbol{\Sigma} = \begin{bmatrix} \boldsymbol{\Sigma}_1 & \boldsymbol{\Sigma}_{121} & \boldsymbol{\Sigma}_{122} \\ \boldsymbol{\Sigma}_{211} & \boldsymbol{\Sigma}_{2n} & \boldsymbol{\Sigma}_{2nm} \\ \boldsymbol{\Sigma}_{212} & \boldsymbol{\Sigma}_{2mn} & \boldsymbol{\Sigma}_{2m} \end{bmatrix} = \begin{bmatrix} \boldsymbol{P}_1 & \boldsymbol{P}_{12} \\ \boldsymbol{P}_{21} & \boldsymbol{P}_2 \end{bmatrix} \tag{12}$$

where $\boldsymbol{\Sigma}_{2m}$ is m-by-m matrix and

$$\boldsymbol{P}_1 = \begin{bmatrix} \boldsymbol{\Sigma}_1 & \boldsymbol{\Sigma}_{121} \\ \boldsymbol{\Sigma}_{211} & \boldsymbol{\Sigma}_{2n} \end{bmatrix},\ \boldsymbol{P}_{21} = \begin{bmatrix} \boldsymbol{\Sigma}_{212} & \boldsymbol{\Sigma}_{2mn} \end{bmatrix},\ \boldsymbol{P}_{12} = \begin{bmatrix} \boldsymbol{\Sigma}_{122} \\ \boldsymbol{\Sigma}_{2nm} \end{bmatrix},\ \boldsymbol{P}_2 = \boldsymbol{\Sigma}_{2m} \tag{13}$$

Then the posterior predictive distribution of $\boldsymbol{x}_{2\,(n+1):(n+m)}$ conditional on $\boldsymbol{x}_{1\,1:(n+m)}$, $\boldsymbol{x}_{2\,1:n}$ and $\boldsymbol{\theta}$ is

$$f(\boldsymbol{x}_{2\,(n+1):(n+m)}|\boldsymbol{x}_{1\,1:(n+m)},\boldsymbol{x}_{2\,1:n},\boldsymbol{\theta}) = (2\pi\sigma^2)^{-m/2}\,|\boldsymbol{R}_{m|n}|^{-1/2} \exp[(-1/2\sigma^2)\,(\boldsymbol{x}_{2\,(n+1):(n+m)} - \boldsymbol{\mu}_{m|n})^{\mathrm{T}}\,\boldsymbol{R}_{m|n}^{-1}\,(\boldsymbol{x}_{2(n+1):(n+m)} - \boldsymbol{\mu}_{m|n})] \tag{14}$$

$$\boldsymbol{\mu}_{m|n} := \mu_2\boldsymbol{e}_m + \boldsymbol{P}_{21}\,\boldsymbol{P}_1^{-1}\,([\boldsymbol{x}_{1\,1:(n+m)}^{\mathrm{T}}\ \boldsymbol{x}_{2\,1:n}^{\mathrm{T}}] - [\mu_1\boldsymbol{e}_{n+m}^{\mathrm{T}}\ \mu_2\boldsymbol{e}_n^{\mathrm{T}}]) \tag{15}$$

$$\boldsymbol{R}_{m|n} := \boldsymbol{P}_2 - \boldsymbol{P}_{21}\,\boldsymbol{P}_1^{-1}\,\boldsymbol{P}_{12} \tag{16}$$

Here we mention that in the following $\boldsymbol{\theta}$ will be considered known and equal to its maximum likelihood estimate. In a Bayesian setting we would assume that $\boldsymbol{\theta}$ is a random variable, but this is out of the scope of this study. In the Bayesian setting the uncertainty of the prediction would increase (see e.g. Tyralis and Koutsoyiannis, 2013a). The variables that will be examined in the following will be considered normal. For truncated normal variables the interested reader is referred to Horrace (2005) and Tyralis and Koutsoyiannis (2013). The examination of non-normal variables is out of the scope of this study as well. For more details on the method and how it is compared to the methods of Krzysztofowicz (1999) and Wang et al. (2009) see Tyralis and Koutsoyiannis (2013b).

5. Methodology

We applied our methodology on global temperature data and precipitation data shown in Table 1. These data are modeled by a Hurst-Kolmogorov process (Koutsoyiannis, 2011, Koutsoyiannis and Montanari, 2007). The deterministic models used in the study were the General Circulation Models (GCMs). We used the 20C3M for the calibration of the model and the SRES scenarios A1B, B1, A2 (Table 2) were taken into consideration for the prediction of the stochastic model. The specific GCMs that where used in the study are shown in Table 3. Tables 4-7 show the maximum likelihood estimates of the bivariate HKp $\{\underline{\boldsymbol{x}}_t = (\underline{x}_{1t},\underline{x}_{2t})\}$, where $\{\underline{x}_{1t}\}$ is the process which models the GCM and $\{\underline{x}_{2t}\}$ is the process which models the observations. The time interval for the calibration spans from the maximum starting year of the corresponding 20C3M scenario and the observed data to the minimum of the corresponding 20C3M scenario and the observed data. We also examined the case where the parameters are estimated separately. Specifically the $\{\underline{x}_{1t}\}$, $\{\underline{x}_{2t}\}$ are assumed to be univariate HKps and their parameters are estimated as in Tyralis and Koutsoyiannis (2011). The sample cross-correlation function is used in this case to estimate ρ.

Using the simultaneous maximum likelihood estimate of ρ, we obtain the posterior predictive distribution of $\underline{\boldsymbol{x}}_{2\,(n+1):(n+m)}$ conditional on $\boldsymbol{x}_{1\,1:(n+m)}$, $\boldsymbol{x}_{2\,1:n}$ and $\boldsymbol{\theta}$ from (14). The other parameters of the bivariate process are estimated again assuming that $\{\underline{x}_{1t}\}$, $\{\underline{x}_{2t}\}$ are univariate HKps, however in this case we use the whole sample, starting from the common starting year of $\{\underline{x}_{1t}\}$ and $\{\underline{x}_{2t}\}$ until the year 2100 for the $\{\underline{x}_{1t}\}$ parameter estimates and the common end year of the corresponding 20C3M scenario and $\{\underline{x}_{2t}\}$ for the $\{\underline{x}_{2t}\}$ parameter estimates. The samples from the posterior predictive probability of $\underline{x}_t|\boldsymbol{x}_n$, $t = n+1, n+2,\ldots$, were used to obtain samples for the variable of interest $\underline{x}_t^{(30)}$ given by (17) following the framework in Koutsoyiannis et al. (2007).

$$\underline{x}_t^{(30)} := (1/30)\Big(\sum_{l=t-29}^{n} x_l + \sum_{l=n+1}^{t} \underline{x}_l\Big),\ t = n+1, \ldots, n+29 \text{ and } \underline{x}_t^{(30)} := (1/30) \sum_{l=t-29}^{t} \underline{x}_l,\ t = n+30, n+31, \ldots \tag{17}$$

6. Examined datasets

Table 2. IPCC scenarios and their relevance to the study.

	Scenario	Characteristics	Reason for being appropriate or inappropriate
AR4	SRES	Various hypothetical scenarios for the future.	Runs start in the 21st century.
	A1B	A future world of very rapid economic growth, low population growth and rapid introduction of new and more efficient technology. Major underlying themes are economic and cultural convergence and capacity building, with a substantial reduction in regional differences in per capita income. In this world, people pursue personal wealth rather than environmental quality.	
	B1	A convergent world with the same global population as in the A1 storyline but with rapid changes in economic structures toward a service and information economy, with reductions in materials intensity, and the introduction of clean and resource-efficient technologies.	
	A2	A very heterogeneous world. The underlying theme is that of strengthening regional cultural identities, with an emphasis on family values and local traditions, high population growth, and less concern for rapid economic development.	
	COMMIT	Greenhouse gases fixed at year 2000 levels.	Runs start in the 21st century, however it is a conservative scenario.
	1%-2X, 1%-4X	Assume a 1%-per-year increase in CO2, usually starting at year 1850.	Results in CO2 being 570 cm³/m³ (ppm) already in 1920, when in fact it was 379 cm³/m³ in 2005. Actual 20th century concentrations are required.
	PI-cntrl	Uses pre-industrial greenhouse gas concentrations.	Actual 20th century concentrations are required.
	20C3M	Generated from output of late 19th & 20th century simulations from coupled ocean–atmosphere models, to help assess past climate change.	This scenario is used for calibration.

Sources: Leggett et al. (1992); Nakicenovic & Swart (1999); Carter et al. (1999); Hegerl et al. (2003); http://www.ipcc-data.org/ar4/gcm_data.html

Table 1. Study historical time series.

Data	Name	Developed by	Time interval	Source
Temperature	Global Land-Ocean Temperature Index	GISS	1880-2012	http://data.giss.nasa.gov
Temperature	Annual Global Land and Ocean Temperature Anomalies	NOAA	1880-2012	http://governmentshutdown.noaa.gov/
Temperature	Combined land [CRUTEM4] and marine temperature anomalies	CRU	1850-2012	http://www.cru.uea.ac.uk/cru/data/temperature/
Precipitation	Precipitation over land areas	CRU	1900-1998	http://www.climatedata.info/Precipitation/Precipitation/global.html

Table 3. Main characteristics of the GCMs used in the study.

IPCC report	Name	Developed by	Country
AR4	BCC CM1	Beijing Climate Center	China
	BCCR BCM2.0	Bjerknes Centre for Climate Research	Norway
	CCSM3.0	National Center for Atmospheric Research	USA
	CGCM3.1 (T47)	Canadian Centre for Climate Modelling & Analysis	Canada
	CGCM3.1 (T63)	Canadian Centre for Climate Modelling & Analysis	Canada
	CNRM CM3	Météo-France / Centre National de Recherches Météorologiques	France
	CSIRO Mk3.5	CSIRO Atmospheric Research	Australia
	ECHAM5 MPI-OM	Max Planck Institute for Meteorology	Germany
	ECHO G	Meteorological Institute of the University of Bonn, Meteorological Research Institute of KMA, and Model and Data group.	Germany/Korea
	FGOALS g1.0	LASG / Institute of Atmospheric Physics	China
	GFDL CM2.1	US Dept. of Commerce / NOAA / Geophysical Fluid Dynamics Laboratory	USA
	GISS ER	NASA / Goddard Institute for Space Studies	USA
	INGV ECHAM4	Instituto Nazionale di Geofisica e Vulcanologia	Italy
	INM CM3.0	Institute for Numerical Mathematics	Russia
	IPSL CM4	Institut Pierre Simon Laplace	France
	MIROC3.2 (medres)	Center for Climate System Research (The University of Tokyo), National Institute for Environmental Studies, and Frontier Research Center for Global Change (JAMSTEC)	Japan
	MRI CGCM 2.3.2	Meteorological Research Institute	Japan
	PCM	National Center for Atmospheric Research	USA
	UKMO HadCM3	Hadley Centre for Climate Prediction and Research / Met Office	UK
	UKMO HadGEM1	Hadley Centre for Climate Prediction and Research / Met Office	UK

Sources: http://www-pcmdi.llnl.gov/ipcc/model_documentation/ipcc_model_documentation.php; climexp.knmi.nl

7. Maximum likelihood estimates for temperature datasets parameters

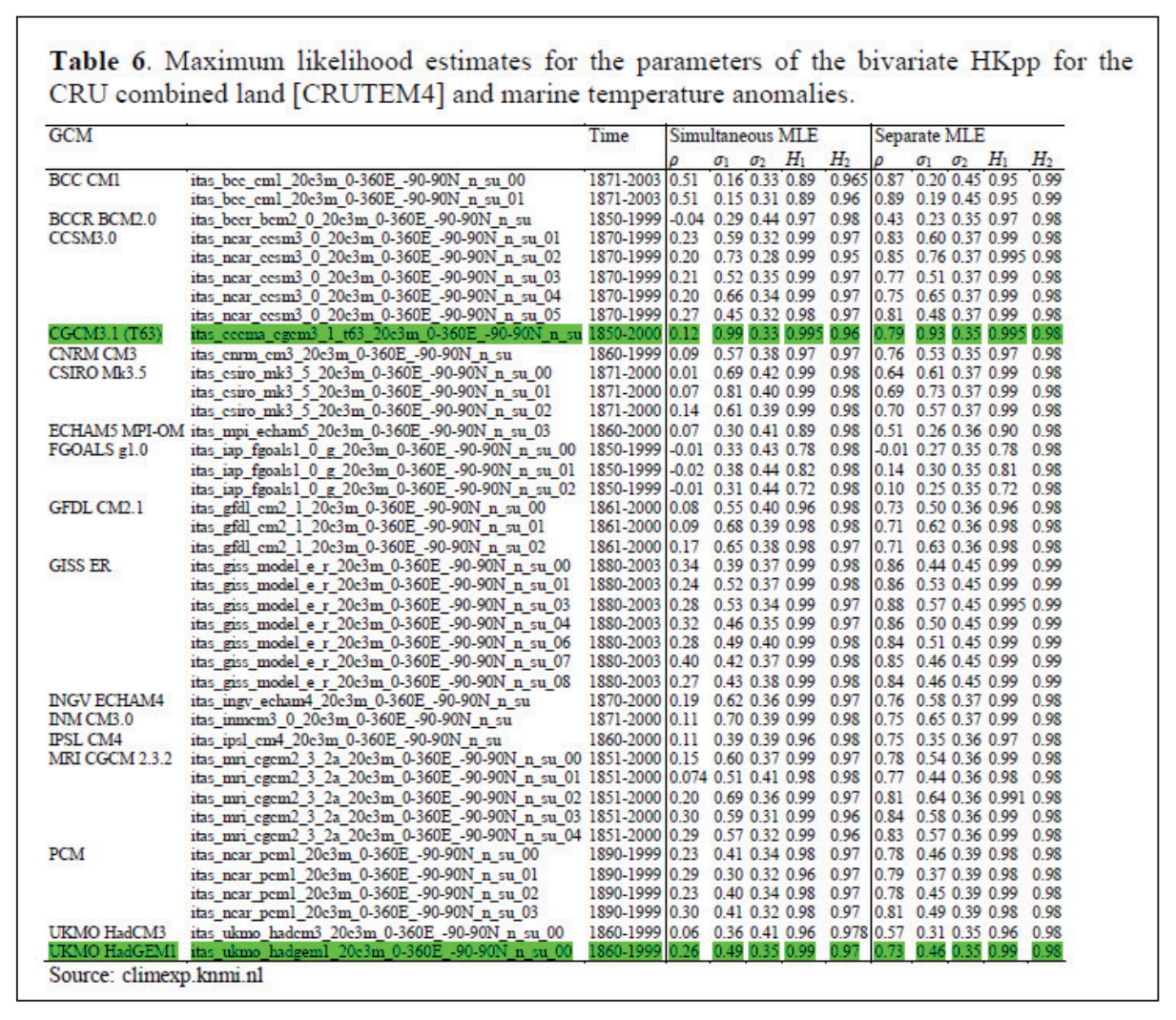

Table 6. Maximum likelihood estimates for the parameters of the bivariate HKpp for the CRU combined land [CRUTEM4] and marine temperature anomalies.

GCM		Time	Simultaneous MLE ρ	σ_1	σ_2	H_1	H_2	Separate MLE ρ	σ_1	σ_2	H_1	H_2
BCC CM1	itas_bcc_cm1_20c3m_0-360E_-90-90N_n_su_00	1871-2003	0.51	0.16	0.33	0.89	0.965	0.87	0.20	0.45	0.95	0.99
	itas_bcc_cm1_20c3m_0-360E_-90-90N_n_su_01	1871-2003	0.51	0.15	0.31	0.89	0.96	0.89	0.19	0.45	0.95	0.99
BCCR BCM2.0	itas_bccr_bcm2_0_20c3m_0-360E_-90-90N_n_su	1850-1999	-0.04	0.29	0.44	0.97	0.98	0.43	0.23	0.35	0.97	0.98
CCSM3.0	itas_ncar_ccsm3_0_20c3m_0-360E_-90-90N_n_su_01	1870-1999	0.23	0.59	0.32	0.99	0.97	0.83	0.60	0.37	0.99	0.98
	itas_ncar_ccsm3_0_20c3m_0-360E_-90-90N_n_su_02	1870-1999	0.20	0.73	0.28	0.99	0.95	0.85	0.76	0.37	0.995	0.98
	itas_ncar_ccsm3_0_20c3m_0-360E_-90-90N_n_su_03	1870-1999	0.21	0.52	0.35	0.99	0.97	0.77	0.51	0.37	0.99	0.98
	itas_ncar_ccsm3_0_20c3m_0-360E_-90-90N_n_su_04	1870-1999	0.20	0.66	0.34	0.99	0.97	0.75	0.65	0.37	0.99	0.98
	itas_ncar_ccsm3_0_20c3m_0-360E_-90-90N_n_su_05	1870-1999	0.27	0.45	0.32	0.98	0.97	0.81	0.48	0.37	0.99	0.98
CGCM3.1 (T63)	itas_cccma_cgcm3_1_t63_20c3m_0-360E_-90-90N_n_su	1850-2000	0.12	0.99	0.33	0.995	0.96	0.79	0.93	0.35	0.995	0.98
CNRM CM3	itas_cnrm_cm3_20c3m_0-360E_-90-90N_n_su	1860-1999	0.09	0.57	0.38	0.97	0.97	0.76	0.53	0.35	0.97	0.98
CSIRO Mk3.5	itas_csiro_mk3_5_20c3m_0-360E_-90-90N_n_su_00	1871-2000	0.01	0.69	0.42	0.99	0.98	0.64	0.61	0.37	0.99	0.98
	itas_csiro_mk3_5_20c3m_0-360E_-90-90N_n_su_01	1871-2000	0.07	0.81	0.40	0.99	0.98	0.69	0.73	0.37	0.99	0.98
	itas_csiro_mk3_5_20c3m_0-360E_-90-90N_n_su_02	1871-2000	0.14	0.61	0.39	0.99	0.98	0.70	0.57	0.37	0.99	0.98
ECHAM5 MPI-OM	itas_mpi_echam5_20c3m_0-360E_-90-90N_n_su_03	1860-2000	0.07	0.30	0.41	0.89	0.98	0.51	0.26	0.36	0.90	0.98
FGOALS g1.0	itas_iap_fgoals1_0_g_20c3m_0-360E_-90-90N_n_su_00	1850-1999	-0.01	0.33	0.43	0.78	0.98	-0.01	0.27	0.35	0.78	0.98
	itas_iap_fgoals1_0_g_20c3m_0-360E_-90-90N_n_su_01	1850-1999	-0.02	0.38	0.44	0.82	0.98	0.14	0.30	0.35	0.81	0.98
	itas_iap_fgoals1_0_g_20c3m_0-360E_-90-90N_n_su_02	1850-1999	-0.01	0.31	0.44	0.72	0.98	0.10	0.25	0.35	0.72	0.98
GFDL CM2.1	itas_gfdl_cm2_1_20c3m_0-360E_-90-90N_n_su_00	1861-2000	0.08	0.55	0.40	0.96	0.98	0.73	0.50	0.36	0.96	0.98
	itas_gfdl_cm2_1_20c3m_0-360E_-90-90N_n_su_01	1861-2000	0.09	0.68	0.39	0.98	0.98	0.71	0.62	0.36	0.98	0.98
	itas_gfdl_cm2_1_20c3m_0-360E_-90-90N_n_su_02	1861-2000	0.17	0.65	0.38	0.98	0.97	0.71	0.63	0.36	0.98	0.98
GISS ER	itas_giss_model_e_r_20c3m_0-360E_-90-90N_n_su_00	1880-2003	0.34	0.39	0.37	0.99	0.98	0.86	0.44	0.45	0.99	0.99
	itas_giss_model_e_r_20c3m_0-360E_-90-90N_n_su_01	1880-2003	0.24	0.52	0.37	0.99	0.98	0.86	0.53	0.45	0.99	0.99
	itas_giss_model_e_r_20c3m_0-360E_-90-90N_n_su_03	1880-2003	0.28	0.53	0.34	0.99	0.97	0.88	0.57	0.45	0.995	0.99
	itas_giss_model_e_r_20c3m_0-360E_-90-90N_n_su_04	1880-2003	0.32	0.46	0.35	0.99	0.97	0.86	0.50	0.45	0.99	0.99
	itas_giss_model_e_r_20c3m_0-360E_-90-90N_n_su_06	1880-2003	0.28	0.49	0.40	0.99	0.98	0.84	0.51	0.45	0.99	0.99
	itas_giss_model_e_r_20c3m_0-360E_-90-90N_n_su_07	1880-2003	0.40	0.42	0.37	0.99	0.98	0.85	0.46	0.45	0.99	0.99
	itas_giss_model_e_r_20c3m_0-360E_-90-90N_n_su_08	1880-2003	0.27	0.43	0.38	0.99	0.98	0.84	0.46	0.45	0.99	0.99
INGV ECHAM4	itas_ingv_echam4_20c3m_0-360E_-90-90N_n_su	1870-2000	0.19	0.62	0.36	0.99	0.97	0.76	0.58	0.37	0.99	0.98
INM CM3.0	itas_inmcm3_0_20c3m_0-360E_-90-90N_n_su	1871-2000	0.11	0.70	0.39	0.99	0.98	0.75	0.65	0.37	0.99	0.98
IPSL CM4	itas_ipsl_cm4_20c3m_0-360E_-90-90N_n_su	1860-2000	0.11	0.39	0.39	0.96	0.98	0.75	0.35	0.36	0.97	0.98
MRI CGCM 2.3.2	itas_mri_cgcm2_3_2a_20c3m_0-360E_-90-90N_n_su_00	1851-2000	0.15	0.60	0.37	0.99	0.97	0.78	0.54	0.36	0.99	0.98
	itas_mri_cgcm2_3_2a_20c3m_0-360E_-90-90N_n_su_01	1851-2000	0.074	0.51	0.41	0.98	0.98	0.77	0.44	0.36	0.98	0.98
	itas_mri_cgcm2_3_2a_20c3m_0-360E_-90-90N_n_su_02	1851-2000	0.20	0.69	0.36	0.99	0.97	0.81	0.64	0.36	0.991	0.98
	itas_mri_cgcm2_3_2a_20c3m_0-360E_-90-90N_n_su_03	1851-2000	0.30	0.59	0.31	0.99	0.96	0.84	0.58	0.36	0.99	0.98
	itas_mri_cgcm2_3_2a_20c3m_0-360E_-90-90N_n_su_04	1851-2000	0.29	0.57	0.32	0.99	0.96	0.83	0.57	0.36	0.99	0.98
PCM	itas_ncar_pcm1_20c3m_0-360E_-90-90N_n_su_00	1890-1999	0.23	0.41	0.34	0.98	0.97	0.78	0.46	0.39	0.98	0.98
	itas_ncar_pcm1_20c3m_0-360E_-90-90N_n_su_01	1890-1999	0.29	0.30	0.32	0.96	0.97	0.79	0.37	0.39	0.98	0.98
	itas_ncar_pcm1_20c3m_0-360E_-90-90N_n_su_02	1890-1999	0.23	0.40	0.34	0.98	0.97	0.78	0.45	0.39	0.99	0.98
	itas_ncar_pcm1_20c3m_0-360E_-90-90N_n_su_03	1890-1999	0.30	0.41	0.32	0.98	0.97	0.81	0.49	0.39	0.98	0.98
UKMO HadCM3	itas_ukmo_hadcm3_20c3m_0-360E_-90-90N_n_su_00	1860-1999	0.06	0.36	0.41	0.96	0.978	0.57	0.31	0.35	0.96	0.98
UKMO HadGEM1	itas_ukmo_hadgem1_20c3m_0-360E_-90-90N_n_su_00	1860-1999	0.26	0.49	0.35	0.99	0.97	0.73	0.46	0.35	0.99	0.98

Source: climexp.knmi.nl

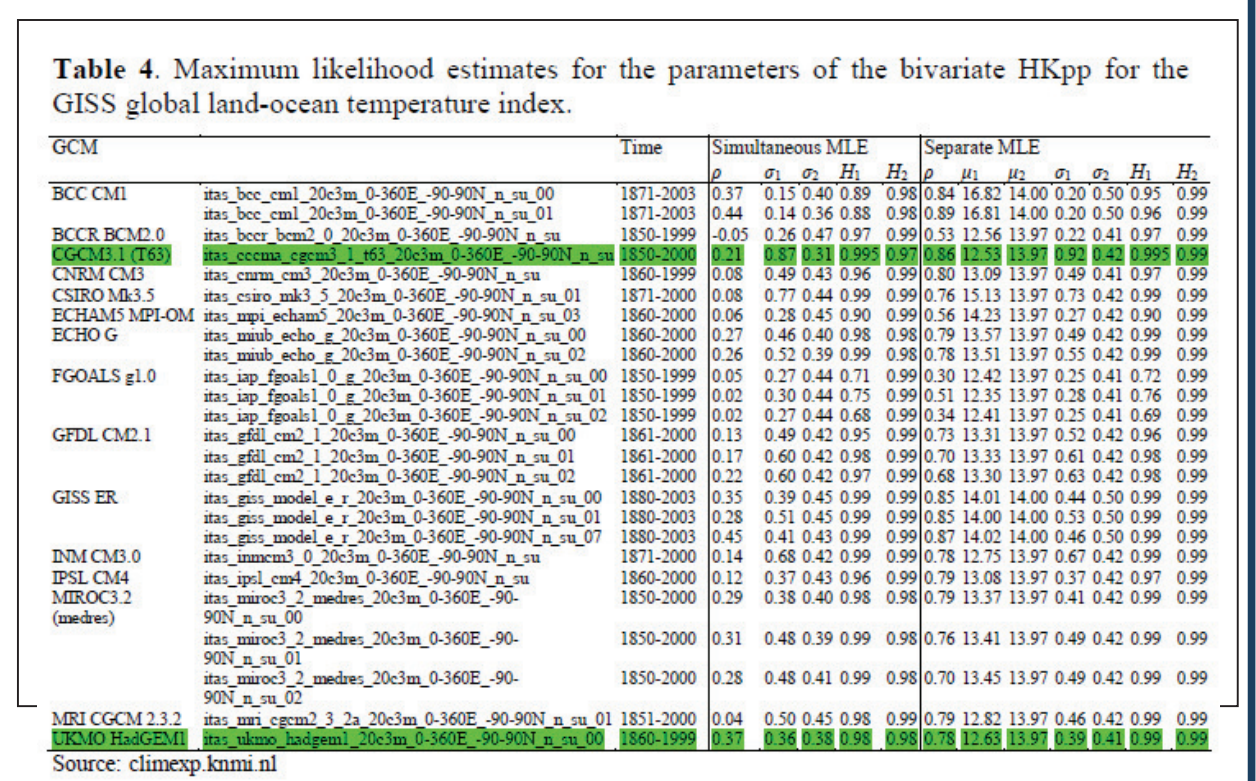

Table 4. Maximum likelihood estimates for the parameters of the bivariate HKpp for the GISS global land-ocean temperature index.

GCM		Time	Simultaneous MLE ρ	σ_1	σ_2	H_1	H_2	Separate MLE ρ	μ_1	μ_2	σ_1	σ_2	H_1	H_2
BCC CM1	itas_bcc_cm1_20c3m_0-360E_-90-90N_n_su_00	1871-2003	0.37	0.15	0.40	0.89	0.98	0.84	16.82	14.00	0.20	0.50	0.95	0.99
	itas_bcc_cm1_20c3m_0-360E_-90-90N_n_su_01	1871-2003	0.44	0.14	0.36	0.88	0.98	0.89	16.81	14.00	0.20	0.50	0.96	0.99
BCCR BCM2.0	itas_bccr_bcm2_0_20c3m_0-360E_-90-90N_n_su	1850-1999	-0.05	0.26	0.47	0.97	0.99	0.53	12.56	13.97	0.22	0.41	0.97	0.99
CGCM3.1 (T63)	itas_cccma_cgcm3_1_t63_20c3m_0-360E_-90-90N_n_su	1850-2000	0.21	0.87	0.31	0.995	0.97	0.86	12.53	13.97	0.92	0.42	0.995	0.99
CNRM CM3	itas_cnrm_cm3_20c3m_0-360E_-90-90N_n_su	1860-1999	0.08	0.49	0.43	0.96	0.99	0.80	13.09	13.97	0.49	0.41	0.97	0.99
CSIRO Mk3.5	itas_csiro_mk3_5_20c3m_0-360E_-90-90N_n_su_01	1871-2000	0.08	0.77	0.44	0.99	0.99	0.76	15.13	13.97	0.73	0.42	0.99	0.99
ECHAM5 MPI-OM	itas_mpi_echam5_20c3m_0-360E_-90-90N_n_su_03	1860-2000	0.06	0.28	0.45	0.90	0.99	0.56	14.23	13.97	0.27	0.42	0.90	0.99
ECHO G	itas_miub_echo_g_20c3m_0-360E_-90-90N_n_su_00	1860-2000	0.27	0.46	0.40	0.98	0.98	0.79	13.57	13.97	0.49	0.42	0.99	0.99
	itas_miub_echo_g_20c3m_0-360E_-90-90N_n_su_02	1860-2000	0.26	0.52	0.39	0.99	0.98	0.78	13.51	13.97	0.55	0.42	0.99	0.99
FGOALS g1.0	itas_iap_fgoals1_0_g_20c3m_0-360E_-90-90N_n_su_00	1850-1999	0.05	0.27	0.44	0.71	0.99	0.30	12.42	13.97	0.25	0.41	0.72	0.99
	itas_iap_fgoals1_0_g_20c3m_0-360E_-90-90N_n_su_01	1850-1999	0.02	0.30	0.44	0.75	0.99	0.51	12.35	13.97	0.28	0.41	0.76	0.99
	itas_iap_fgoals1_0_g_20c3m_0-360E_-90-90N_n_su_02	1850-1999	0.02	0.27	0.44	0.68	0.99	0.34	12.41	13.97	0.25	0.41	0.69	0.99
GFDL CM2.1	itas_gfdl_cm2_1_20c3m_0-360E_-90-90N_n_su_00	1861-2000	0.13	0.49	0.42	0.95	0.99	0.73	13.31	13.97	0.52	0.42	0.96	0.99
	itas_gfdl_cm2_1_20c3m_0-360E_-90-90N_n_su_01	1861-2000	0.17	0.60	0.42	0.98	0.99	0.70	13.33	13.97	0.61	0.42	0.98	0.99
	itas_gfdl_cm2_1_20c3m_0-360E_-90-90N_n_su_02	1861-2000	0.22	0.60	0.42	0.97	0.99	0.68	13.30	13.97	0.63	0.42	0.98	0.99
GISS ER	itas_giss_model_e_r_20c3m_0-360E_-90-90N_n_su_00	1880-2003	0.35	0.39	0.45	0.99	0.99	0.85	14.01	14.00	0.44	0.50	0.99	0.99
	itas_giss_model_e_r_20c3m_0-360E_-90-90N_n_su_01	1880-2003	0.28	0.51	0.45	0.99	0.99	0.85	14.00	14.00	0.53	0.50	0.99	0.99
	itas_giss_model_e_r_20c3m_0-360E_-90-90N_n_su_07	1880-2003	0.45	0.41	0.43	0.99	0.99	0.87	14.02	14.00	0.46	0.50	0.99	0.99
INM CM3.0	itas_inmcm3_0_20c3m_0-360E_-90-90N_n_su	1871-2000	0.14	0.68	0.42	0.99	0.99	0.78	12.75	13.97	0.67	0.42	0.99	0.99
IPSL CM4	itas_ipsl_cm4_20c3m_0-360E_-90-90N_n_su	1860-2000	0.12	0.37	0.43	0.96	0.99	0.79	13.08	13.97	0.37	0.42	0.97	0.99
MIROC3.2 (medres)	itas_miroc3_2_medres_20c3m_0-360E_-90-90N_n_su_00	1850-2000	0.29	0.38	0.40	0.98	0.98	0.79	13.37	13.97	0.41	0.42	0.99	0.99
	itas_miroc3_2_medres_20c3m_0-360E_-90-90N_n_su_01	1850-2000	0.31	0.48	0.39	0.99	0.98	0.76	13.41	13.97	0.49	0.42	0.99	0.99
	itas_miroc3_2_medres_20c3m_0-360E_-90-90N_n_su_02	1850-2000	0.28	0.48	0.41	0.99	0.98	0.70	13.45	13.97	0.49	0.42	0.99	0.99
MRI CGCM 2.3.2	itas_mri_cgcm2_3_2a_20c3m_0-360E_-90-90N_n_su_01	1851-2000	0.04	0.50	0.45	0.98	0.99	0.79	12.82	13.97	0.46	0.42	0.99	0.99
UKMO HadGEM1	itas_ukmo_hadgem1_20c3m_0-360E_-90-90N_n_su_00	1860-1999	0.37	0.36	0.38	0.98	0.98	0.78	12.63	13.97	0.39	0.41	0.99	0.99

Source: climexp.knmi.nl

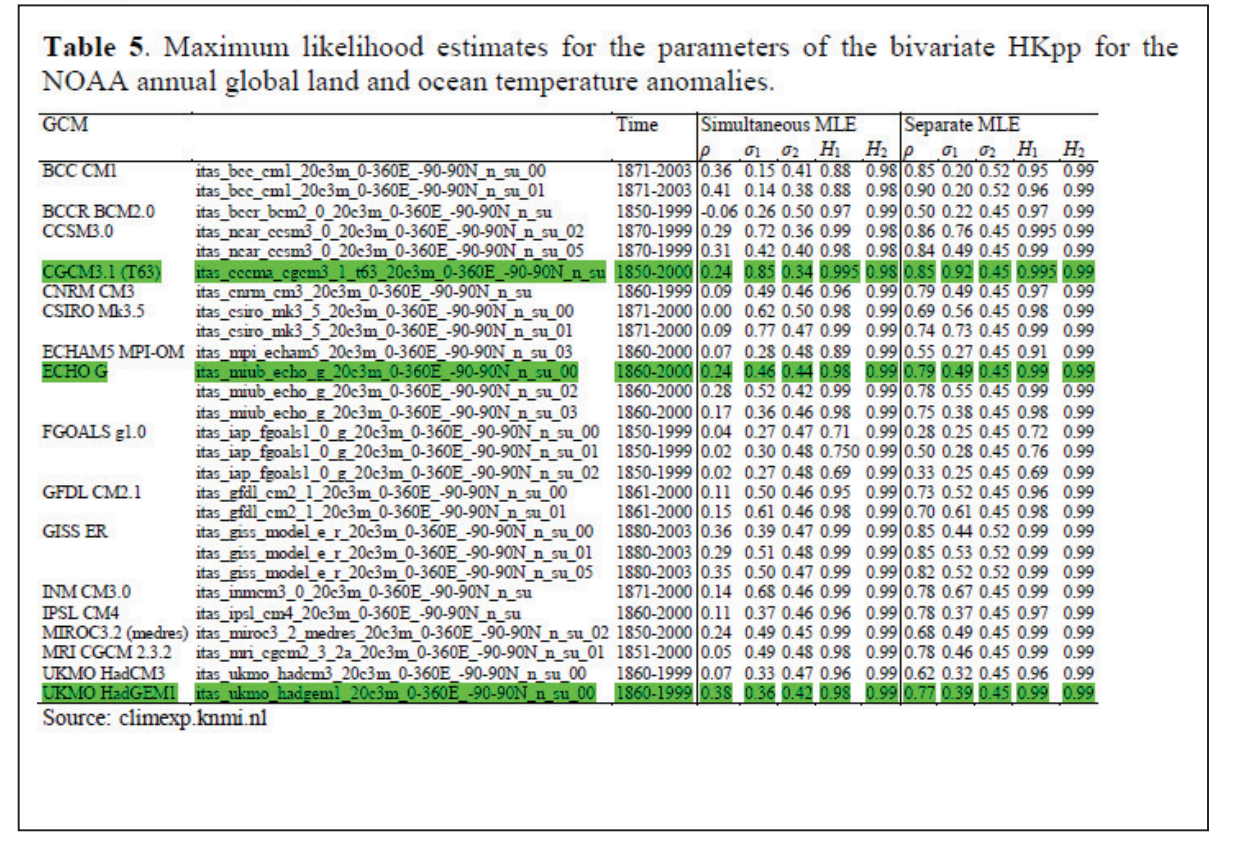

Table 5. Maximum likelihood estimates for the parameters of the bivariate HKpp for the NOAA annual global land and ocean temperature anomalies.

GCM		Time	Simultaneous MLE ρ	σ_1	σ_2	H_1	H_2	Separate MLE ρ	σ_1	σ_2	H_1	H_2
BCC CM1	itas_bcc_cm1_20c3m_0-360E_-90-90N_n_su_00	1871-2003	0.36	0.15	0.41	0.88	0.98	0.85	0.20	0.52	0.95	0.99
	itas_bcc_cm1_20c3m_0-360E_-90-90N_n_su_01	1871-2003	0.41	0.14	0.38	0.88	0.98	0.90	0.20	0.52	0.96	0.99
BCCR BCM2.0	itas_bccr_bcm2_0_20c3m_0-360E_-90-90N_n_su	1850-1999	-0.06	0.26	0.50	0.97	0.99	0.50	0.22	0.45	0.97	0.99
CCSM3.0	itas_ncar_ccsm3_0_20c3m_0-360E_-90-90N_n_su_02	1870-1999	0.29	0.72	0.36	0.99	0.98	0.86	0.76	0.45	0.995	0.99
	itas_ncar_ccsm3_0_20c3m_0-360E_-90-90N_n_su_05	1870-1999	0.31	0.42	0.40	0.98	0.98	0.84	0.49	0.45	0.99	0.99
CGCM3.1 (T63)	itas_cccma_cgcm3_1_t63_20c3m_0-360E_-90-90N_n_su	1850-2000	0.24	0.85	0.34	0.995	0.98	0.85	0.92	0.45	0.995	0.99
CNRM CM3	itas_cnrm_cm3_20c3m_0-360E_-90-90N_n_su	1860-1999	0.09	0.49	0.46	0.96	0.99	0.79	0.49	0.45	0.97	0.99
CSIRO Mk3.5	itas_csiro_mk3_5_20c3m_0-360E_-90-90N_n_su_00	1871-2000	0.00	0.62	0.50	0.98	0.99	0.69	0.56	0.45	0.98	0.99
	itas_csiro_mk3_5_20c3m_0-360E_-90-90N_n_su_01	1871-2000	0.09	0.77	0.47	0.99	0.99	0.74	0.73	0.45	0.99	0.99
ECHAM5 MPI-OM	itas_mpi_echam5_20c3m_0-360E_-90-90N_n_su_03	1860-2000	0.07	0.28	0.48	0.89	0.99	0.55	0.27	0.45	0.91	0.99
ECHO G	itas_miub_echo_g_20c3m_0-360E_-90-90N_n_su_00	1860-2000	0.24	0.46	0.44	0.98	0.99	0.79	0.49	0.45	0.99	0.99
	itas_miub_echo_g_20c3m_0-360E_-90-90N_n_su_02	1860-2000	0.28	0.52	0.42	0.99	0.99	0.78	0.55	0.45	0.99	0.99
	itas_miub_echo_g_20c3m_0-360E_-90-90N_n_su_03	1860-2000	0.17	0.36	0.46	0.98	0.99	0.75	0.38	0.45	0.98	0.99
FGOALS g1.0	itas_iap_fgoals1_0_g_20c3m_0-360E_-90-90N_n_su_00	1850-1999	0.04	0.27	0.47	0.71	0.99	0.28	0.25	0.45	0.72	0.99
	itas_iap_fgoals1_0_g_20c3m_0-360E_-90-90N_n_su_01	1850-1999	0.02	0.30	0.48	0.750	0.99	0.50	0.28	0.45	0.76	0.99
	itas_iap_fgoals1_0_g_20c3m_0-360E_-90-90N_n_su_02	1850-1999	0.02	0.27	0.48	0.69	0.99	0.33	0.25	0.45	0.69	0.99
GFDL CM2.1	itas_gfdl_cm2_1_20c3m_0-360E_-90-90N_n_su_00	1861-2000	0.11	0.50	0.46	0.95	0.99	0.73	0.52	0.45	0.96	0.99
	itas_gfdl_cm2_1_20c3m_0-360E_-90-90N_n_su_01	1861-2000	0.15	0.61	0.46	0.98	0.99	0.70	0.61	0.45	0.98	0.99
GISS ER	itas_giss_model_e_r_20c3m_0-360E_-90-90N_n_su_00	1880-2003	0.36	0.39	0.47	0.99	0.99	0.85	0.44	0.52	0.99	0.99
	itas_giss_model_e_r_20c3m_0-360E_-90-90N_n_su_01	1880-2003	0.29	0.51	0.48	0.99	0.99	0.85	0.53	0.52	0.99	0.99
	itas_giss_model_e_r_20c3m_0-360E_-90-90N_n_su_05	1880-2003	0.35	0.50	0.47	0.99	0.99	0.82	0.52	0.52	0.99	0.99
INM CM3.0	itas_inmcm3_0_20c3m_0-360E_-90-90N_n_su	1871-2000	0.14	0.68	0.46	0.99	0.99	0.78	0.67	0.45	0.99	0.99
IPSL CM4	itas_ipsl_cm4_20c3m_0-360E_-90-90N_n_su	1860-2000	0.11	0.37	0.46	0.96	0.99	0.78	0.37	0.45	0.97	0.99
MIROC3.2 (medres)	itas_miroc3_2_medres_20c3m_0-360E_-90-90N_n_su_02	1850-2000	0.24	0.49	0.45	0.99	0.99	0.68	0.49	0.45	0.99	0.99
MRI CGCM 2.3.2	itas_mri_cgcm2_3_2a_20c3m_0-360E_-90-90N_n_su_01	1851-2000	0.05	0.49	0.48	0.98	0.99	0.78	0.46	0.45	0.99	0.99
UKMO HadCM3	itas_ukmo_hadcm3_20c3m_0-360E_-90-90N_n_su_00	1860-1999	0.07	0.33	0.47	0.96	0.99	0.62	0.32	0.45	0.96	0.99
UKMO HadGEM1	itas_ukmo_hadgem1_20c3m_0-360E_-90-90N_n_su_00	1860-1999	0.38	0.36	0.42	0.98	0.99	0.77	0.39	0.45	0.99	0.99

Source: climexp.knmi.nl

Highlighted are the cases whose results were used at Figures 1-12

8. Maximum likelihood estimates for the precipitation dataset parameters

Highlighted are the cases whose results were used at Figures 1-12

Separate MLEs are not used in the study, because the parameters are not orthogonal

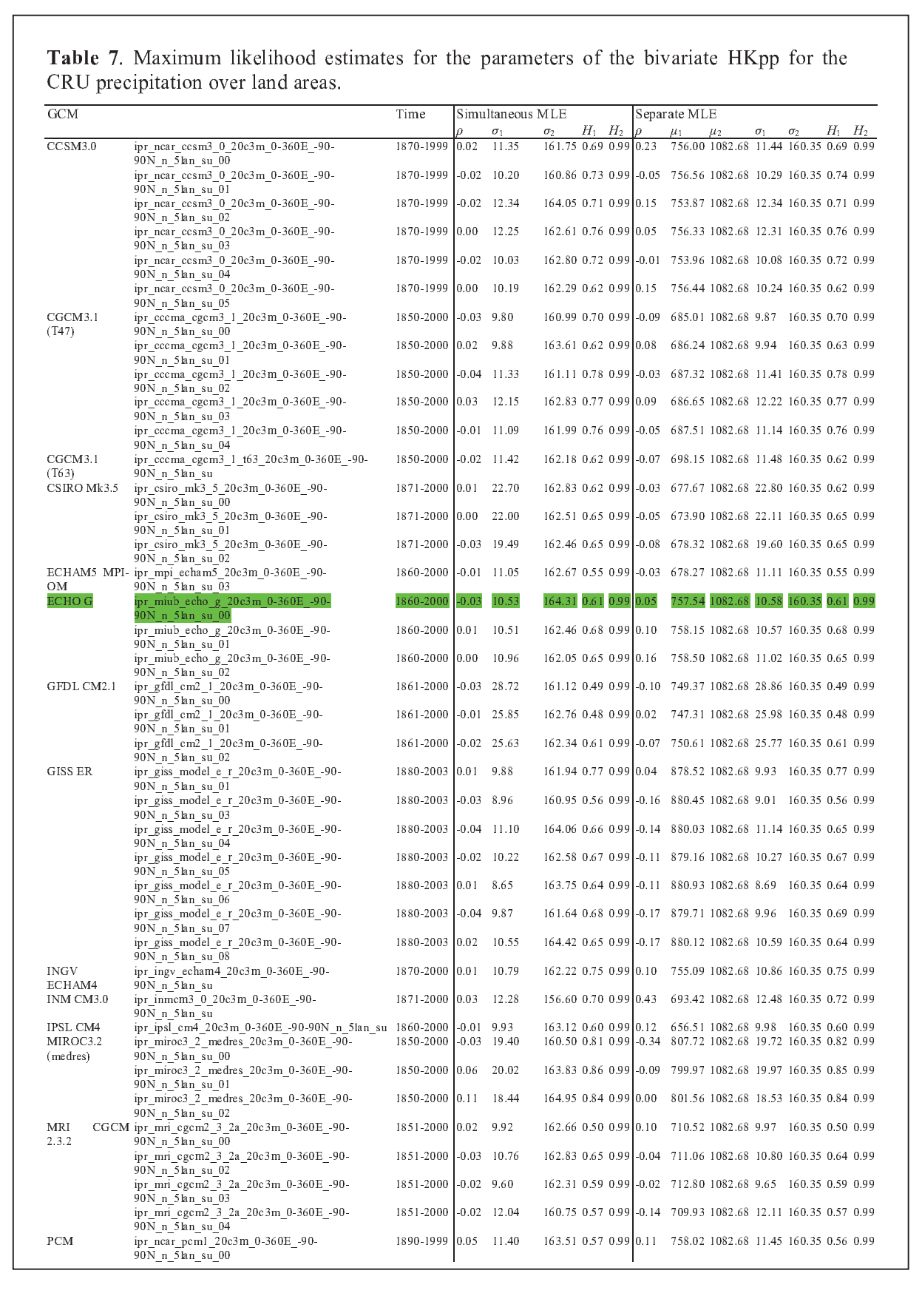

Table 7. Maximum likelihood estimates for the parameters of the bivariate HKpp for the CRU precipitation over land areas.

GCM		Time	Simultaneous MLE ρ	σ_1	σ_2	H_1	H_2	Separate MLE ρ	μ_1	μ_2	σ_1	σ_2	H_1	H_2
CCSM3.0	ipr_ncar_ccsm3_0_20c3m_0-360E_-90-90N_n_5lan_su_00	1870-1999	0.02	11.35	161.75	0.69	0.99	0.23	756.00	1082.68	11.44	160.35	0.69	0.99
	ipr_ncar_ccsm3_0_20c3m_0-360E_-90-90N_n_5lan_su_01	1870-1999	-0.02	10.20	160.86	0.73	0.99	-0.05	756.56	1082.68	10.29	160.35	0.74	0.99
	ipr_ncar_ccsm3_0_20c3m_0-360E_-90-90N_n_5lan_su_02	1870-1999	-0.02	12.34	164.05	0.71	0.99	0.15	753.87	1082.68	12.34	160.35	0.71	0.99
	ipr_ncar_ccsm3_0_20c3m_0-360E_-90-90N_n_5lan_su_03	1870-1999	0.00	12.25	162.61	0.76	0.99	0.05	756.33	1082.68	12.31	160.35	0.76	0.99
	ipr_ncar_ccsm3_0_20c3m_0-360E_-90-90N_n_5lan_su_04	1870-1999	-0.02	10.03	162.80	0.72	0.99	-0.01	753.96	1082.68	10.08	160.35	0.72	0.99
	ipr_ncar_ccsm3_0_20c3m_0-360E_-90-90N_n_5lan_su_05	1870-1999	0.00	10.19	162.29	0.62	0.99	0.15	756.44	1082.68	10.24	160.35	0.62	0.99
CGCM3.1 (T47)	ipr_cccma_cgcm3_1_20c3m_0-360E_-90-90N_n_5lan_su_00	1850-2000	-0.03	9.80	160.99	0.70	0.99	-0.09	685.01	1082.68	9.87	160.35	0.70	0.99
	ipr_cccma_cgcm3_1_20c3m_0-360E_-90-90N_n_5lan_su_01	1850-2000	0.02	9.88	163.61	0.62	0.99	0.08	686.24	1082.68	9.94	160.35	0.63	0.99
	ipr_cccma_cgcm3_1_20c3m_0-360E_-90-90N_n_5lan_su_02	1850-2000	-0.04	11.33	161.11	0.78	0.99	-0.03	687.32	1082.68	11.41	160.35	0.78	0.99
	ipr_cccma_cgcm3_1_20c3m_0-360E_-90-90N_n_5lan_su_03	1850-2000	0.03	12.15	162.83	0.77	0.99	0.09	686.65	1082.68	12.22	160.35	0.77	0.99
	ipr_cccma_cgcm3_1_20c3m_0-360E_-90-90N_n_5lan_su_04	1850-2000	-0.01	11.09	161.99	0.76	0.99	-0.05	687.51	1082.68	11.14	160.35	0.76	0.99
CGCM3.1 (T63)	ipr_cccma_cgcm3_1_t63_20c3m_0-360E_-90-90N_n_5lan_su	1850-2000	-0.02	11.42	162.18	0.62	0.99	-0.07	698.15	1082.68	11.48	160.35	0.62	0.99
CSIRO Mk3.5	ipr_csiro_mk3_5_20c3m_0-360E_-90-90N_n_5lan_su_00	1871-2000	0.01	22.70	162.83	0.62	0.99	-0.03	677.67	1082.68	22.80	160.35	0.62	0.99
	ipr_csiro_mk3_5_20c3m_0-360E_-90-90N_n_5lan_su_01	1871-2000	0.00	22.00	162.51	0.65	0.99	-0.05	673.90	1082.68	22.11	160.35	0.65	0.99
	ipr_csiro_mk3_5_20c3m_0-360E_-90-90N_n_5lan_su_02	1871-2000	-0.03	19.49	162.46	0.65	0.99	-0.08	678.32	1082.68	19.60	160.35	0.65	0.99
ECHAM5 MPI-OM	ipr_mpi_echam5_20c3m_0-360E_-90-90N_n_5lan_su_03	1860-2000	-0.01	11.05	162.67	0.55	0.99	-0.03	678.27	1082.68	11.11	160.35	0.55	0.99
ECHO G	ipr_miub_echo_g_20c3m_0-360E_-90-90N_n_5lan_su_00	1860-2000	-0.03	10.53	164.31	0.61	0.99	0.05	757.54	1082.68	10.58	160.35	0.61	0.99
	ipr_miub_echo_g_20c3m_0-360E_-90-90N_n_5lan_su_01	1860-2000	0.01	10.51	162.46	0.68	0.99	0.10	758.15	1082.68	10.57	160.35	0.68	0.99
	ipr_miub_echo_g_20c3m_0-360E_-90-90N_n_5lan_su_02	1860-2000	0.00	10.96	162.05	0.65	0.99	0.16	758.50	1082.68	11.02	160.35	0.65	0.99
GFDL CM2.1	ipr_gfdl_cm2_1_20c3m_0-360E_-90-90N_n_5lan_su_00	1861-2000	-0.03	28.72	161.12	0.49	0.99	-0.10	749.37	1082.68	28.86	160.35	0.49	0.99
	ipr_gfdl_cm2_1_20c3m_0-360E_-90-90N_n_5lan_su_01	1861-2000	-0.01	25.85	162.76	0.48	0.99	0.02	747.31	1082.68	25.98	160.35	0.48	0.99
	ipr_gfdl_cm2_1_20c3m_0-360E_-90-90N_n_5lan_su_02	1861-2000	-0.02	25.63	162.34	0.61	0.99	-0.07	750.61	1082.68	25.77	160.35	0.61	0.99
GISS ER	ipr_giss_model_e_r_20c3m_0-360E_-90-90N_n_5lan_su_01	1880-2003	0.01	9.88	161.94	0.77	0.99	0.04	878.52	1082.68	9.93	160.35	0.77	0.99
	ipr_giss_model_e_r_20c3m_0-360E_-90-90N_n_5lan_su_03	1880-2003	-0.03	8.96	160.95	0.56	0.99	-0.16	880.45	1082.68	9.01	160.35	0.56	0.99
	ipr_giss_model_e_r_20c3m_0-360E_-90-90N_n_5lan_su_04	1880-2003	-0.04	11.10	164.06	0.66	0.99	-0.14	880.03	1082.68	11.14	160.35	0.65	0.99
	ipr_giss_model_e_r_20c3m_0-360E_-90-90N_n_5lan_su_05	1880-2003	-0.02	10.22	162.58	0.67	0.99	-0.11	879.16	1082.68	10.27	160.35	0.67	0.99
	ipr_giss_model_e_r_20c3m_0-360E_-90-90N_n_5lan_su_06	1880-2003	0.01	8.65	163.75	0.64	0.99	-0.11	880.93	1082.68	8.69	160.35	0.64	0.99
	ipr_giss_model_e_r_20c3m_0-360E_-90-90N_n_5lan_su_07	1880-2003	-0.04	9.87	161.64	0.68	0.99	-0.17	879.71	1082.68	9.96	160.35	0.69	0.99
	ipr_giss_model_e_r_20c3m_0-360E_-90-90N_n_5lan_su_08	1880-2003	0.02	10.55	164.42	0.65	0.99	-0.17	880.12	1082.68	10.59	160.35	0.64	0.99
INGV ECHAM4	ipr_ingv_echam4_20c3m_0-360E_-90-90N_n_5lan_su	1870-2000	0.01	10.79	162.22	0.75	0.99	0.10	755.09	1082.68	10.86	160.35	0.75	0.99
INM CM3.0	ipr_inmcm3_0_20c3m_0-360E_-90-90N_n_5lan_su	1871-2000	0.03	12.28	156.60	0.70	0.99	0.43	693.42	1082.68	12.48	160.35	0.72	0.99
IPSL CM4	ipr_ipsl_cm4_20c3m_0-360E_-90-90N_n_5lan_su	1860-2000	-0.01	9.93	163.12	0.60	0.99	0.12	656.51	1082.68	9.98	160.35	0.60	0.99
MIROC3.2 (medres)	ipr_miroc3_2_medres_20c3m_0-360E_-90-90N_n_5lan_su_00	1850-2000	-0.03	19.40	160.50	0.81	0.99	-0.34	807.72	1082.68	19.72	160.35	0.82	0.99
	ipr_miroc3_2_medres_20c3m_0-360E_-90-90N_n_5lan_su_01	1850-2000	0.06	20.02	163.83	0.86	0.99	-0.09	799.97	1082.68	19.97	160.35	0.85	0.99
	ipr_miroc3_2_medres_20c3m_0-360E_-90-90N_n_5lan_su_02	1850-2000	0.11	18.44	164.95	0.84	0.99	0.00	801.56	1082.68	18.53	160.35	0.84	0.99
MRI CGCM 2.3.2	ipr_mri_cgcm2_3_2a_20c3m_0-360E_-90-90N_n_5lan_su_00	1851-2000	0.02	9.92	162.66	0.50	0.99	0.10	710.52	1082.68	9.97	160.35	0.50	0.99
	ipr_mri_cgcm2_3_2a_20c3m_0-360E_-90-90N_n_5lan_su_02	1851-2000	-0.03	10.76	162.83	0.65	0.99	-0.04	711.06	1082.68	10.80	160.35	0.64	0.99
	ipr_mri_cgcm2_3_2a_20c3m_0-360E_-90-90N_n_5lan_su_03	1851-2000	-0.02	9.60	162.31	0.59	0.99	-0.02	712.80	1082.68	9.65	160.35	0.59	0.99
	ipr_mri_cgcm2_3_2a_20c3m_0-360E_-90-90N_n_5lan_su_04	1851-2000	-0.02	12.04	160.75	0.57	0.99	-0.14	709.93	1082.68	12.11	160.35	0.57	0.99
PCM	ipr_ncar_pcm1_20c3m_0-360E_-90-90N_n_5lan_su_00	1890-1999	0.05	11.40	163.51	0.57	0.99	0.11	758.02	1082.68	11.45	160.35	0.56	0.99

9. Confidence regions for future climate

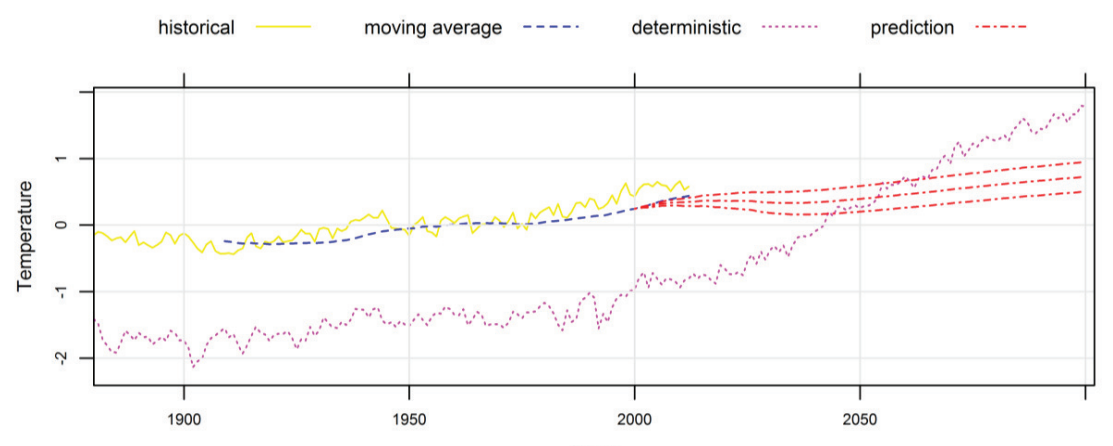

Figure 1. 95% confidence region for the predictive 30-moving average temperature (°C) for the A1B scenario of the ECHO-G model, using the NOAA annual global land and ocean temperature anomalies.

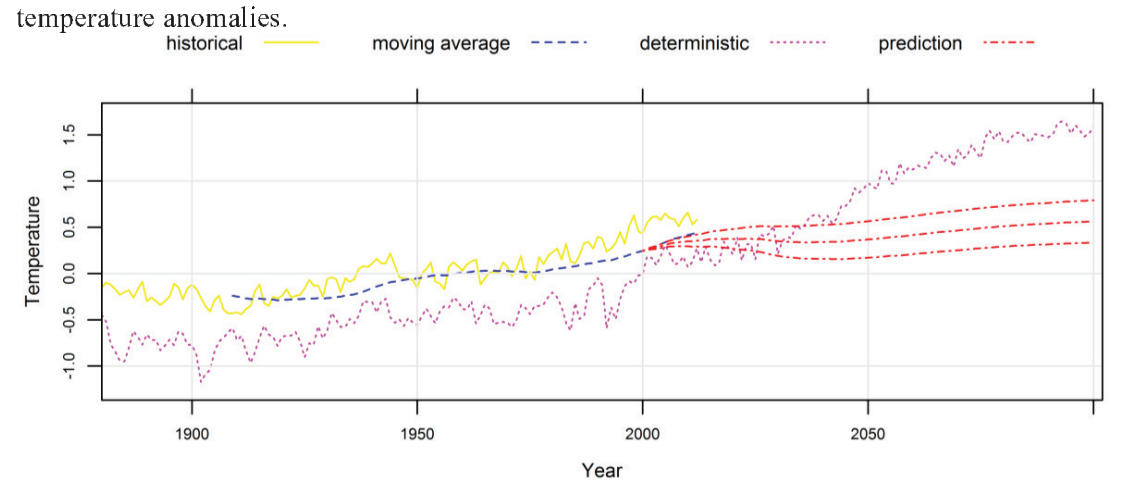

Figure 2. 95% confidence region for the predictive 30-moving average temperature (°C) for the B1 scenario of the ECHO-G model, using the NOAA annual global land and ocean temperature anomalies.

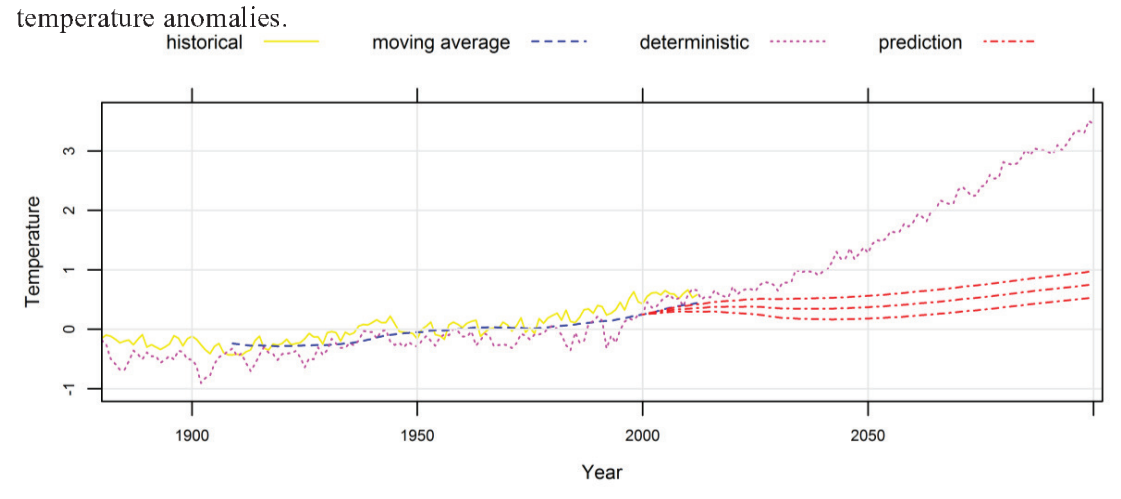

Figure 3. 95% confidence region for the predictive 30-moving average temperature (°C) for the A2 scenario of the ECHO-G model, using the NOAA annual global land and ocean temperature anomalies.

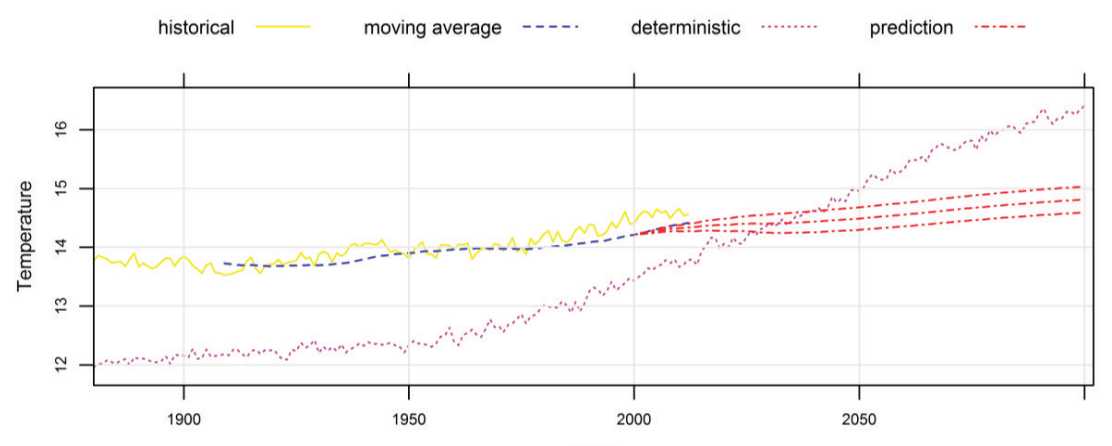

Figure 4. 95% confidence region for the predictive 30-moving average temperature (°C) for the A1B scenario of the CGCM3.1 (T63) model, using the GISS global land-ocean temperature index.

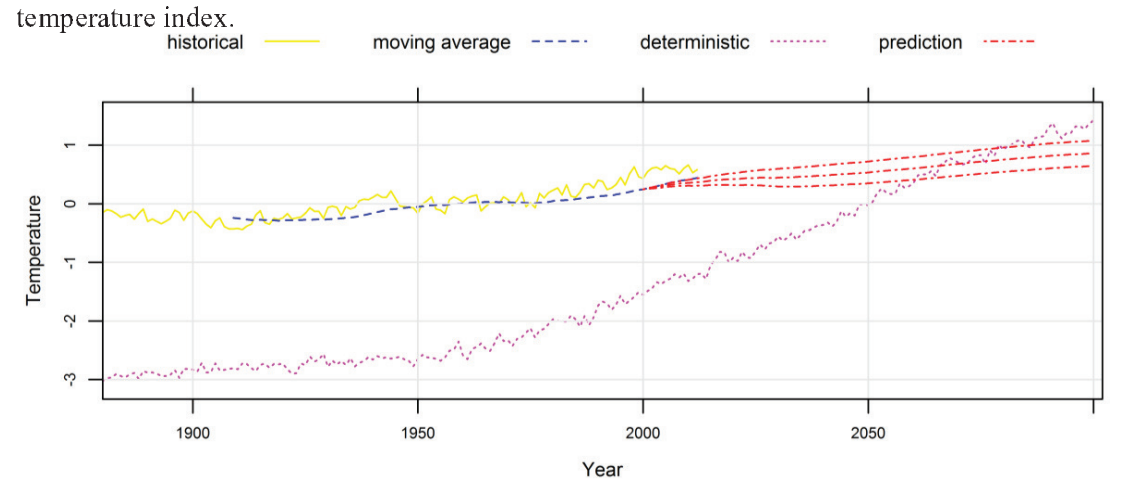

Figure 5. 95% confidence region for the predictive 30-moving average temperature (°C) for the A1B scenario of the CGCM3.1 (T63) model, using the NOAA annual global land and ocean temperature anomalies.

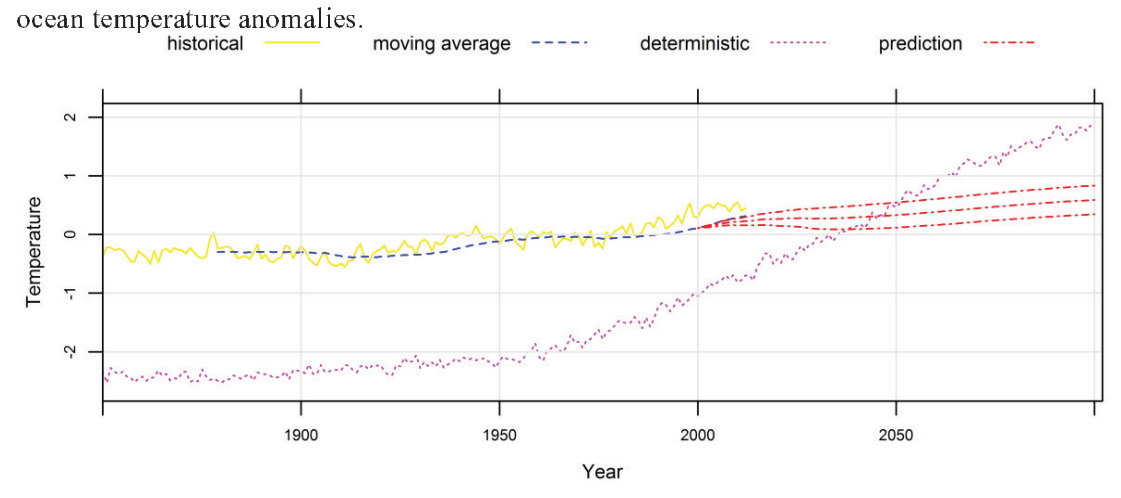

Figure 6. 95% confidence region for the predictive 30-moving average temperature (°C) for the A1B scenario of the CGCM3.1 (T63) model, using the CRU combined land [CRUTEM4] and marine temperature anomalies.

10. Confidence regions for future climate

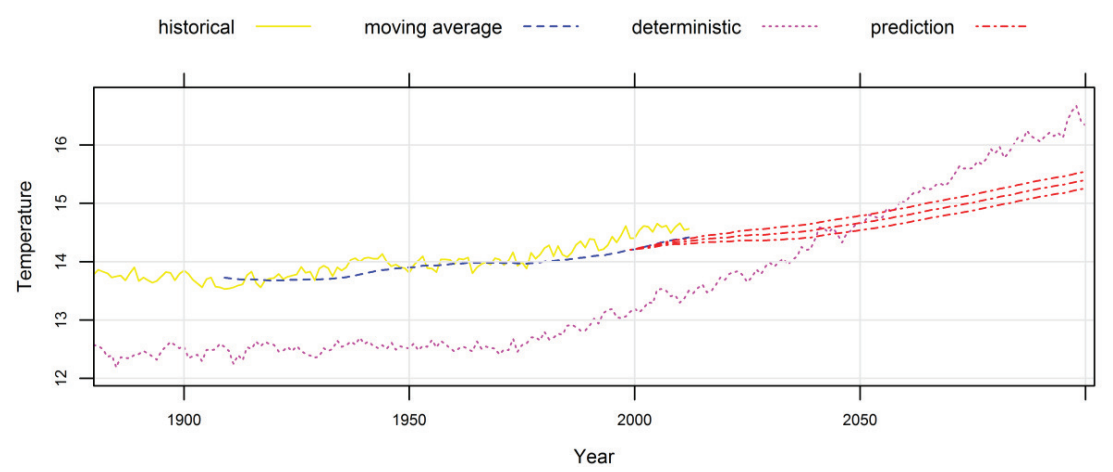

Figure 7. 95% confidence region for the predictive 30-moving average temperature (°C) for the A1B scenario of the UKMO HadGEM1 model, using the GISS global land-ocean temperature index.

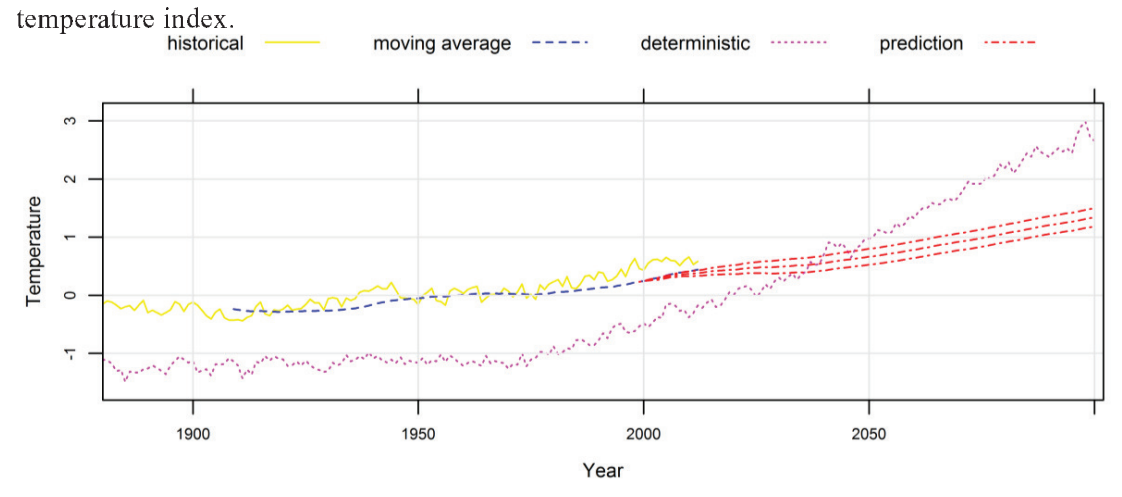

Figure 8. 95% confidence region for the predictive 30-moving average temperature (°C) for the A1B scenario of the UKMO HadGEM1 model, using the NOAA annual global land and ocean temperature anomalies.

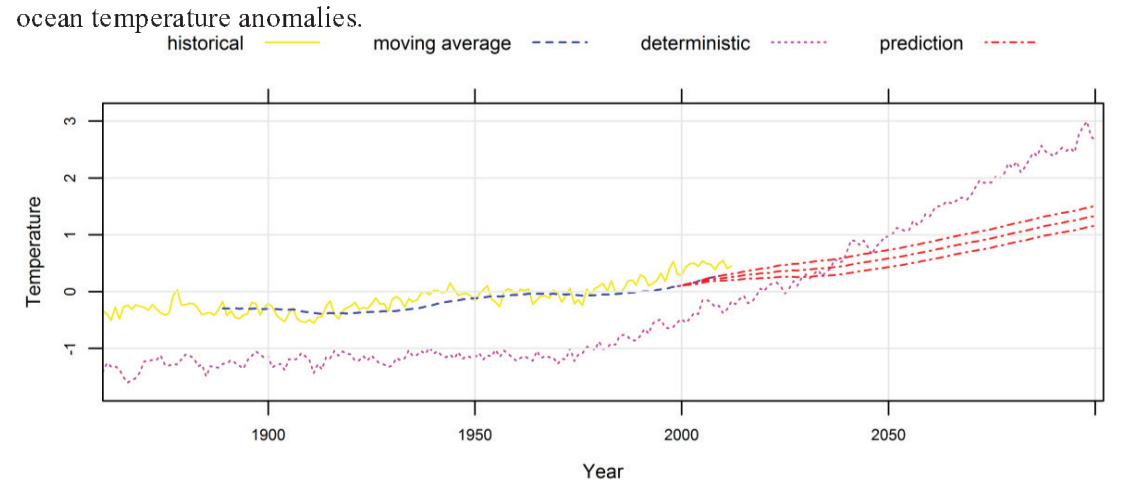

Figure 9. 95% confidence region for the predictive 30-moving average temperature (°C) for the A1B scenario of the UKMO HadGEM1 model, using the CRU combined land [CRUTEM4] and marine temperature anomalies.

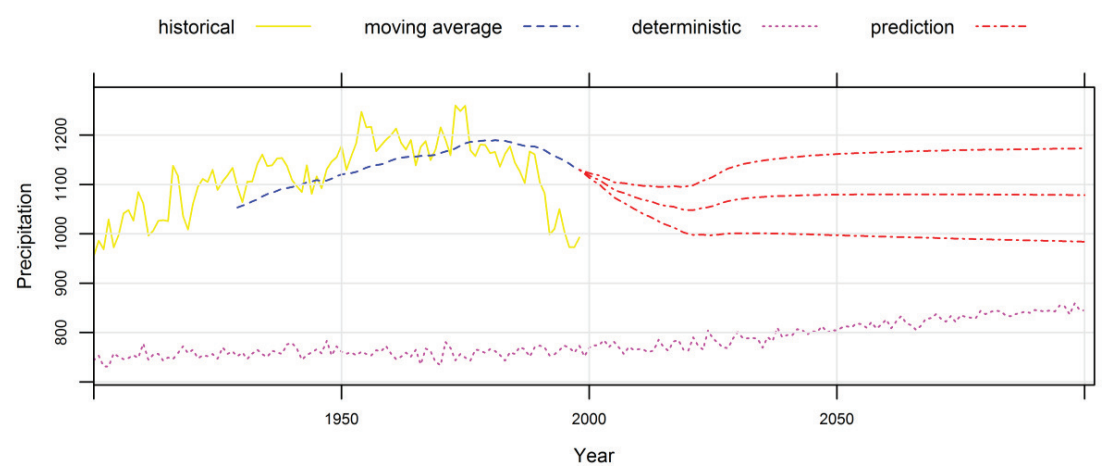

Figure 10. 95% confidence region for the predictive 30-moving average precipitation (mm) for the A1B scenario of the ECHO-G model, using the CRU precipitation over land areas.

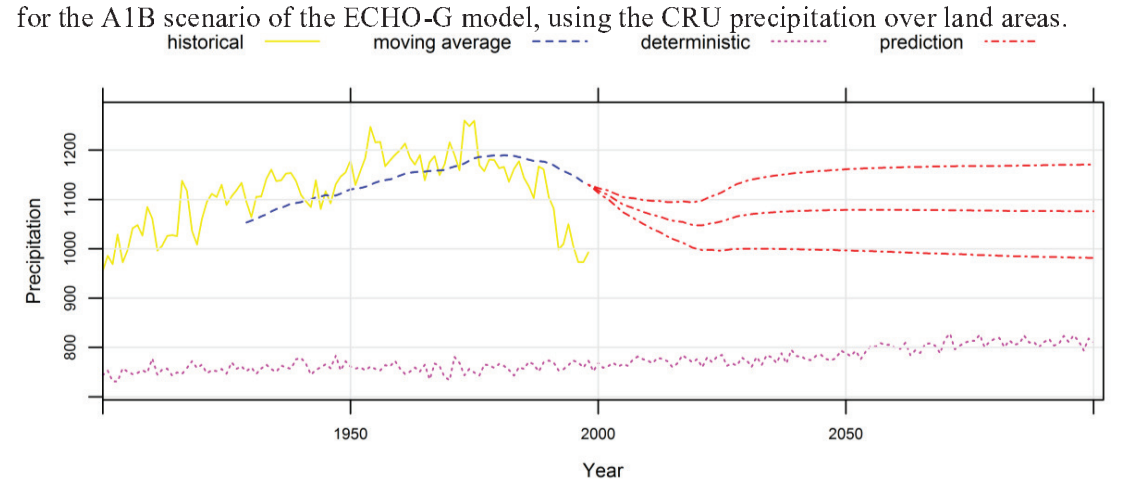

Figure 11. 95% confidence region for the predictive 30-moving average precipitation (mm) for the B1 scenario of the ECHO-G model, using the CRU precipitation over land areas.

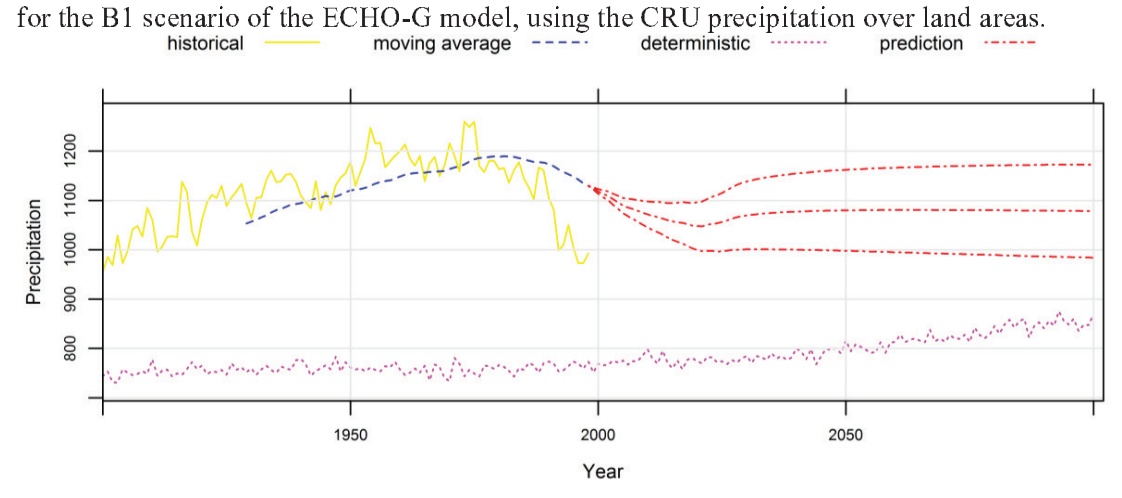

Figure 12. 95% confidence region for the predictive 30-moving average precipitation (mm) for the A2 scenario of the ECHO-G model, using the CRU precipitation over land areas.

11. Conclusions

- We derive a new estimator for the parameters of the bivariate HKp.
- After modelling the observed datasets and the output of GCMs using the bivariate HKp we estimate the parameters of the process.
- Using the estimated values of the parameters we provide stochastic prediction of the future climate combining the projections of the GCMs and their corresponding hindcasts with the observed time series.
- The estimated values of the cross-correlation between the historical datasets (at global scale) and the hindcasts of the GCMs range from 0 to 0.4, showing that the information added by the GCMs to that contained in the historical datasets is not substantial.
- The upper bound of the 95% confidence region of the climatic value of temperature at year 2100 is estimated to about 1°C more than the current value of this climatic variable.
- For the precipitation dataset the estimated value of the cross-correlations between the historical datasets and the hindcasts of the GCMs is almost equal to 0. This means that the output of the GCM has no effect on the stochastic predictions.
- We emphasize that the estimation of the stochastic model parameters should better be performed using only data that were not used in the GCM fitting/tuning, i.e. for the period after 2000. This would correspond to the so-called split-sample technique, which avoids possible model overfitting on the available data. However this would increase considerably the uncertainty of the estimators of the parameters of the models and practically would result in total neglect of the GCM predictions. Hence we decided to approach the problem more conservatively.
- Our approach is an extension of previous studies, which exploited the outputs of deterministic models combined with historical dataset, on persistent stochastic processes.

12. References

- Amblard PO, Coeurjolly JF, Lavancier F, Philippe A (2012) Basic properties of the multivariate fractional Brownian motion. arXiv:1007.0828v2
- Carter TR, Hulme M, Lal M (1999) Guidelines on the use of scenario data for climate impact and adaptation assessment, task group on scenarios for climate impact assessment. Intergovernmental Panel on Climate Change
- Hegerl G, Meehl G, Covey C, Latif M, McAvaney B, Stouffer R (2003) 20C3M: CMIP collecting data from 20th century coupled model simulations. Exchanges 26, 8(1), Int. CLIVAR Project Office
- Horrace W (2005) Some results on the multivariate truncated normal distribution. Journal of Multivariate Analysis 94(1):209-221. doi:10.1016/j.jmva.2004.10.007
- Koutsoyiannis D (2011) Hurst-Kolmogorov dynamics and uncertainty. JAWRA Journal of the American Water Resources Association 47(3):481-495. doi:10.1111/j.1752-1688.2011.00543.x
- Koutsoyiannis D, Efstratiadis A, Georgakakos KP (2007) Uncertainty Assessment of Future Hydroclimatic Predictions: A Comparison of Probabilistic and Scenario-Based Approaches. Journal of Hydrometeorology 8(3):261-281. doi:10.1175/JHM576.1
- Koutsoyiannis D, Montanari A (2007) Statistical analysis of hydroclimatic time series: Uncertainty and insights. Water Resources Research 43(5) W05429. doi:10.1029/2006WR005592
- Krzysztofowicz R (1999) Bayesian Forecasting via Deterministic Model. Risk Analysis 19(4):739-749. doi:10.1111/j.1539-6924.1999.tb00443.x
- Leggett J, Pepper WJ, Swart RJ (1992) Emissions scenarios for the IPCC: an update. In: Climate Change 1992: The Supplementary Report to the IPCC Scientific Assessment (ed. by J. T. Houghton, B. A. Callander & S. K. Varney), 75–95. Cambridge University Press, Cambridge, UK
- Nakicenovic N, Swart R (eds) (1999) IPCC Special Report on Emissions Scenarios. Intergovernmental Panel on Climate Change. Available online at: http://www.grida.no/publications/other/ipcc_sr/?src=/climate/ipcc/emission/
- Tyralis H, Koutsoyiannis D (2011) Simultaneous estimation of the parameters of the Hurst-Kolmogorov stochastic process. Stochastic Environmental Research & Risk Assessment 25(1):21-33. doi:10.1007/s00477-010-0408-x
- Tyralis H, Koutsoyiannis D (2013a) A Bayesian statistical model for deriving the predictive distribution of hydroclimatic variables. Climate Dynamics. doi:10.1007/s00382-013-1804-y
- Tyralis H, Koutsoyiannis D (2013b) On the prediction of persistent processes using the output of deterministic models. (in preparation)
- Wang QJ, Robertson DE, Chiew FHS (2009) A Bayesian joint probability modeling approach for seasonal forecasting of streamflows at multiple sites. Water Resources Research 45(5). doi:10.1029/2008WR007355
- Wei WWS (2006) Time Series Analysis, Univariate and Multivariate Methods. second edition, Pearson Addison Wesley, Chichester